A RANSAC-based 3D line projection fitting:

Supplementary Materials to the paper "A Unified Model for Line Projections in Catadioptric Cameras with Rotationally Symmetric Mirrors"

Pedro Miraldo
Mitsubishi Electric Research Labs (MERL)
miraldo@merl.com

José Pedro Iglesias
Chalmers University of Technology
jose.iglesias@chalmers.se

The main paper focuses on deriving a new unified model for 3D line projection in catadioptric cameras. However, the experimental results show some line-image fittings. Although this is not the paper's main contribution, the fitting of line images in the image of general catadioptric cameras was never shown before. These supplementary materials describe the fitting technique used. First, we explain our RANSAC-based line fitting in more detail and show some figures with the obtained results with synthetic data. Then, as shown in the main document, we offer the advantages of having a unified model instead of previous techniques in the presence of small misalignments.

MATLAB *scripts with all our derivations and with some results shown in this supplementary materials are available at https://github.com/pmiraldo/line-projection-catadioptric.*

A. Line-image fitting

Since line projection in general catadioptric cameras is generally modeled by high degree polynomial equations (implicit functions), getting its coefficients do not work in practice, namely when noisy data is used. Instead, we derive a method that takes into account the general non-center properties of the catadioptric cameras to compute the coefficients of the $\mathcal{I}(u,v)$ by estimating a 3D line and applying the derivations of the paper (Thm. 3 in the main document).

This subsection presents our RANSAC-based line-image fitting technique. The method is a simple technique that builds on the standard RANdom SAmple Consensus method (RANSAC) [5]. As mentioned above, instead of obtaining the polynomial coefficients from the 2D image pixels that are images of a 3D line, we compute its 3D coordinates. As known, 3D lines have four degrees of freedom [9]. It is also known that each line intersection gives one algebraic constraint. (See the general epipolar geometry in constraint in [8].) Then, for non-central systems, the use of four pixels per line image is enough to get its 3D parameters. Each pixel gets a 3D projection ray; with four, we can compute the 3D line passing through them using [10].

With the details presented in the previous paragraph and our line-image derivations ($\mathcal{I}(u,v)$ in Theorem 3), our RANSAC-based line-image fitting is derived as follows. We consider a RANSAC cycle, in which, for each iteration:

1. Since a minimum of four pixels is needed for estimating the 3D line coordinates, we start by sampling a set of four pixels that are potential images of a line, (u_i, v_i) for $i = 1, 2, 3, 4$, and compute the four inverse projection ray corresponding to each of the four pixels $(\mathbf{d}_i, \mathbf{m}_i)$, again for $i = 1, 2, 3, 4$. For that, we need camera system parameters A, B, C, c_2, c_3, $\mathbf{R}$, and $\mathbf{K}$;

2. Using [10], we compute the 3D line parameters that pass through the set of lines $(\mathbf{d}_i, \mathbf{m}_i)$ for $i = 1, 2, 3, 4$;

3. Using the estimated 3D line in the previous step, we compute the line image-hypothesis $\mathcal{I}(u,v) = 0$, using Thm. 3 in the main paper;

4. We do inlier counting using $\mathcal{I}(u,v) = 0$, by computing a distance between the pixels in the image (line image candidates) to the curve. The ones with a value smaller than a defined threshold are considered inliers.

We repeat the process a certain number of iterations, and the final line-image $\mathcal{I}(u,v)$ is given by the hypothesis that obtained the largest number of inliers.

We run some evaluation tests using synthetic data to validate the proposed line-fitting method. We start with a simple example using a catadioptric camera with a spherical mirror: $A = 1$, $B = 0$, $C = 150$, $c_2 = 4$, $c_3 = 25$, with the internal perspective camera parameters indicated in the main document. To generate the synthetic data, we follow the same steps as the ones shown in the main document. In addition, for a 3D line, we sample 500 points and project them into the image using the method in [1]. Then, we add noise to the projected points; a normal distribution with a standard deviation of 1 pixel was used. To conclude, we add 50 outliers to the image. All image points coordinates are rounded up to have (integer) image pixels. For the

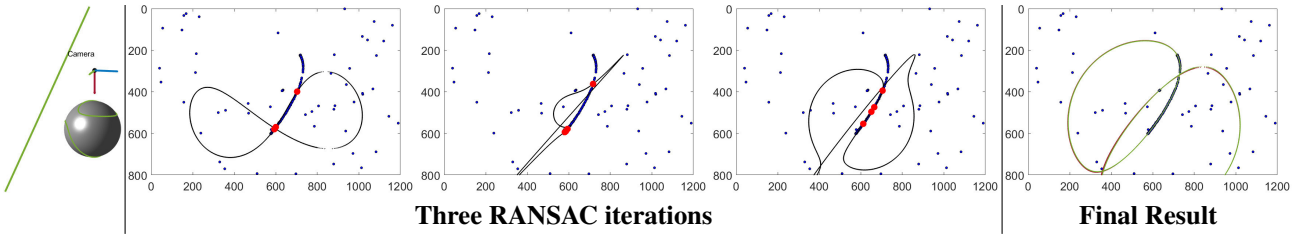

Figure A.1. Running example of the proposed RANSAC-based 3D line projection fitting method. From left to right, we show the used spherical catadioptric system; three RANSAC iteration examples where red points represent the sample pixels, the black curve is the respective hypothesis for $\mathcal{I}(u, v)$; and, at the right, the final result (green curve is the ground truth and red curve depicts the estimated line projection).

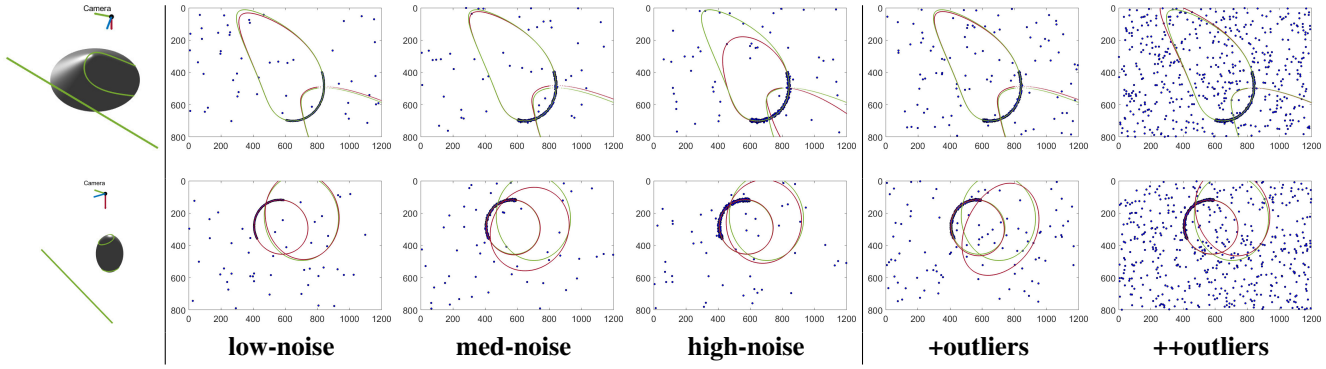

Figure A.2. We show the results of our RANSAC-based line image fitting with different noise levels and number of outliers. The catadioptric systems used were the general and the parabolic, described in the main document. As in Fig. A.1, the red curve is the one estimated by our method; green is the ground-truth 3D line projection. On the left, we show the used system.

RANSAC loop, we consider 1000 iterations and use 2 pixels as a distance threshold for the inlier counting. Results are shown in Fig. A.1.

Next, we run a few more experiments using two of the systems presented in the main paper (See Tab. 2 in the main document), with different outliers and noise levels. Three different levels of noise are considered:

- **low-noise:** corresponding to 1 pixel of standard deviation;
- **med-noise:** corresponding to 3 pixels of standard deviation; and
- **high-noise:** corresponding to 5 pixels of standard deviation

Then, for the **med-noise**, we consider three different numbers of outliers:

- **+outliers:** 100 pixels; and
- **++outliers:** 500 pixels.

We use the same RANSAC cycle settings presented in the previous paragraph, with the inliers threshold equal to 2 pixels. Results are shown in Fig. A.2. From this figure, we can conclude that the 3D line projection fitting technique works well. Even with high noise levels and many outliers, the estimator can get an almost perfect fit of the projected points. As we can see, all the curves representing the image of the mirror sheet where the reflection occurs are matched correctly. Only in the challenging general case for high noise is the curve not perfectly matched due to noise and the fact that this part of the curve represents points where the line terminates at infinity. Still, all the projected points corresponding to the line image are correctly fitted. We also want to highlight that these 3D coordinates of the lines are being estimated with only minimal data. As known, getting the 3D line coordinates from a single catadioptric image is a very challenging problem, especially in estimating the depths of the lines (see [4, 6, 7]). Still, we show in these results that we can have satisfactory line-image fittings using minimal data and RANSAC by estimating the 3D coordinates of a line. For improvement concerning 3D estimation, the next step would be to take all the inliers from our method and run [4, 6].

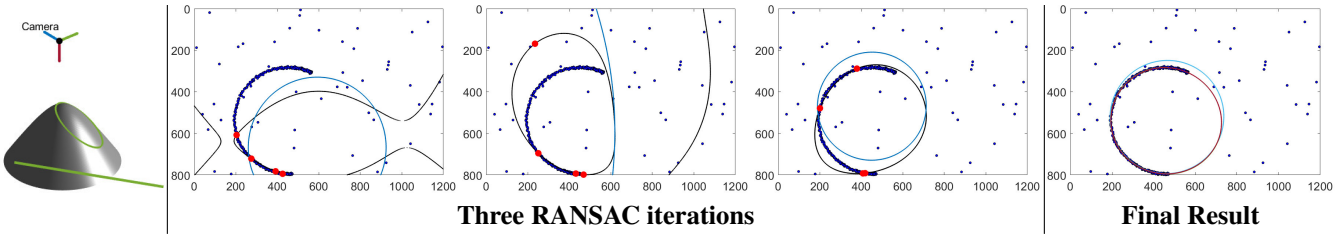

Figure B.3. Running example like Fig. A.1, but considering a central hyperbolic catadioptric system with a misalignment of 5% in y–axis. On the left, we show the used catadioptric system. Then, we present three RANSAC iterations where red points represent the sample pixels, the black curves represent the projection of a 3D line using our unified model $\mathcal{I}(u, v)$, and the blue curves represent the projection of the 3D line using the specific model defined in the literature [2, 3]. At the right is the final result. In red, we show our result, which is overlapped with the ground-truth, in green. Finally, the best model using the model in the literature is shown in cyan.

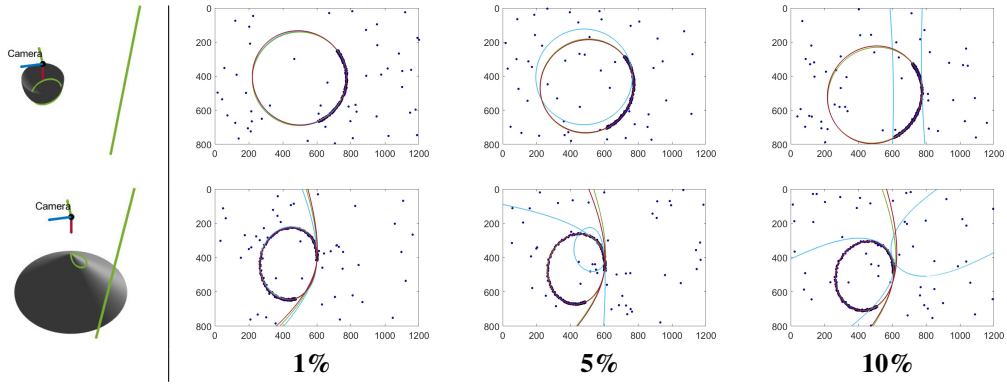

Figure B.4. This figure shows the final results of running the RANSAC-based fitting technique using our unified model against the previously derived specific models in [2, 3], with misalignments of 1%, 5%, and 10%. As in Fig. B.3, red and cyan curves represent the outputs of our RANSAC-based line fittings, using our unified model and the previous methods, respectively. The green curve is the ground truth.

B. Exact vs. approximate modelings

We further motivate the need for unifying modeling for line projection instead of specific modelings [2, 3]. We consider the same setup shown in the main document again, in which we consider systems with small misalignments. Finally, we run the fitting technique defined in the last section.

As before, we sample 500 image points in the line and use the **med-noise** and 50 outliers. We take the specific systems shown in the main document (Tab. 2 at the main document) and run in parallel the RANSAC described in the previous section and a similar one that, instead of using the proposed unified projection model, uses the current method in the literature for the 3D projection of lines. As in the main document, to motivate the need for having a unified model, we use a central hyperbolic catadioptric camera and a minor misalignment of 5% in the y–axis. The results are shown in Fig. B.3, where we show some iterations of the RANSAC cycle and the final result. The first thing one notices is that the curves generated from the previously defined specific model (in blue), since they consist of approximations, do not pass through the image of the four sampled points (in red) – the curve generated from the unified model in black pass through the respective image pixels. Concerning the final results at the right of Fig. B.3, we see clearly that, while our method in red fits perfectly the points and the ground truth curve (in green – overlapped), the one using the previously defined specific catadioptric systems projections (curve in cyan) is significantly deviated and do not fit all the projected points.

To conclude, we show different results with our unified model vs. approximate modelings in the literature, considering different noise levels and misalignment. We consider:

- **1%** of misalignment;
- **5%** of misalignment;
- **10%** of misalignment.

The results for two different systems in Tab. 2 of the main document are shown in Fig. B.4. We can see that, even though for deviations of only 1%, the results are still acceptable for the fitting with previous specific models (marginally the same for the ellipsoidal system), increasing

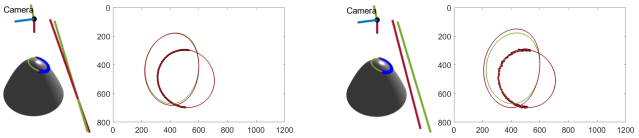

Figure C.5. Green curves in the image and lines in the 3D represent the GT. Red curves and lines are the estimated projection curve and 3D line. Blue points represent the 2D points used in the estimation. We show results for **low-noise** and **high-noise** at the left and right, as described in the supplementary materials.

the variation to 5% is enough for these models to fail in the line-image fitting. For 10% of deviation, previous models do not work. On the other hand, our unified modeling works as expected.

C. 3D line estimation accuracy

Getting the 3D coordinates of a line from a line-image in non-central catadioptric systems is very challenging. Figure C.5 shows some results for two levels of noise. We followed the line fitting technique described above. We show two noise levels and observe that, in general, RANSAC handles this problem well, and the 3D estimates are reasonable. As expected, we get worse 3D estimates when the portion of the line visible in the image reduces significantly or when the camera/line configuration gets near a degenerative case.

References

[1] Amit Agrawal, Yuichi Taguchi, and Srikumar Ramalingam. Beyond Alhazen's problem: Analytical projection model for non-central catadioptric cameras with quadric mirrors. In *CVPR*, pages 2993–3000, 2011. 1

[2] Joao P. Barreto and Helder Araujo. Issues on the geometry of central catadioptric image formation. In *CVPR*, volume 2, pages 422–427, 2001. 3

[3] Jesus Bermudez-Cameo, Gonzalo Lopez-Nicolas, and Jose J. Guerrero. Fitting line projections in non-central catadioptric cameras with revolution symmetry. *CVIU*, 167:134–152, 2018. 3

[4] Vincenzo Caglioti and Simone Gasparini. On the localization of straight lines in 3d space from single 2d images. In *CVPR*, pages 1129–1134, 2005. 2

[5] Martin A. Fischler and Robert C. Bolles. Random sample consensus: A paradigm for model fitting with applications to image analysis and automated cartography. *Commun. ACM*, 24(6):381–395, 1981. 1

[6] Simone Gasparini and Vincenzo Caglioti. Line localization from single catadioptric images. *IJCV*, 94(3):361–374, 2011. 2

[7] Douglas Lanman, Megan Wachs, Gabriel Taubin, and Fernando Cukierman. Reconstructing a 3d line from a single catadioptric image. In *3DPVT*, pages 89–96, 2006. 2

[8] Robert Pless. Using many cameras as one. In *CVPR*, volume 2, 2003. 1

[9] Helmut Pottmann and Johannes Wallner. *Computational Line Geometry*. Springer-Verlag, Berlin, Heidelberg, 2001. 1

[10] Seth Teller and Michael Hohmeyer. Determining the lines through four lines. *J. Graphics Tools*, 4(3):11–22, 1999. 1